Numerical study of laser wake field generated by two colliding laser beams

K. Nagashima, J. Koga, and M. Kando
Advanced Photon Research Center, Japan Atomic Energy Research Institute, Umemidai 8-1, Kizu-cyo, Souraku-gun, Kyoto-fu 619-0215, Japan
(Received 30 July 2001; published 19 November 2001)

The laser wake field generated by two colliding laser beams has been studied numerically. The wake field amplitude is enhanced by a counterpropagating long pulse laser, which has an appropriate frequency difference, and becomes an order of magnitude larger than that of the standard wake field. The field amplitude increases in proportion to the pumping laser intensities until it saturates under the wave breaking limit. The details of the enhanced wake field have been examined at the saturated state.

DOI: 10.1103/PhysRevE.64.066403 PACS number(s): 52.38.−r, 41.75.Lx, 52.75.Di, 52.65.Rr

Recently, significant progress has been made in laser-plasma interactions for generating large electric fields in order to accelerate charged particles. The ponderomotive force of the intense laser pulse excites a longitudinal electron plasma wave (EPW) with a phase velocity close to the speed of light [1]. Since the induced electric field is a few orders of magnitude larger than the accelerating fields in conventional accelerators, it is very attractive for compact particle accelerators. Up to now, three mechanisms have been considered to excite the EPW. They are the laser beat wave (LBW) [2,3], the laser wake field (LWF) [4], and the self-modulated laser wake field (SM-LWF) [5–9]. Many experiments have been performed to observe the excited EPW [10–12] and the accelerated particles [8,9].

In the LBW, two laser pulses are used with a frequency difference equal to the electron plasma frequency $\omega_p = (e^2 n_e / m_e \varepsilon_0)^{1/2}$. This can generate a large amplitude EPW. However, a precise tuning of the laser frequencies and electron density is needed. In the LWF, a single short pulse laser is injected into the plasma where the longitudinal ponderomotive force excites the EPW. The amplitude of the EPW is maximum at the laser pulse length $L \approx \lambda_p/2$ where λ_p is the plasma wavelength, $\lambda_p = 2\pi c/\omega_p$. In the SM-LWF, an intense laser pulse, with pulse length longer than the plasma wavelength, is modulated at the plasma frequency through the Raman forward scattering instability [13–15]. In this method, a large amplitude EPW has been excited and an electric field over 100 GV/m has been observed [6]. However, the field amplitude and its phase cannot be controlled because it grows from an instability. Since the SM-LWF is excited at high electron density, the dephasing distance (where the phase between the particles and the accelerating field slips) is reduced.

For practical accelerators, the accelerating field must be stable and predictable. Therefore, the accelerating length and the field strength have to be controlled without delicate tuning of the laser and plasma parameters. Furthermore, the Lorentz factor γ_{ph} corresponding to the phase velocity of the wave v_{ph} is expected to be high because the maximum attainable electron energy is $W_d \approx 2\gamma_{\mathrm{ph}}^2 m_e c^2$ [where $\gamma_{\mathrm{ph}} = (1 - v_{\mathrm{ph}}^2/c^2)^{-1/2}$] due to the dephasing limit [1], which prefers low density operation. Recently, a new method was proposed for generating a large amplitude wake field using two colliding laser beams with the appropriate frequency difference [16]. One of the laser beams is a short pulse, of which the pulse length is shorter than the plasma wavelength, and the other is a long pulse propagating in the counter direction. The intensities of these pulses are relatively low ($\sim 10^{16}$ W/cm^2) compared to those in the standard LWF or the SM-LWF, and no precise frequency tuning is needed.

Here, the details of the laser wake field generated by two colliding laser beams are examined using one-dimensional PIC simulation code [17]. This is a self-consistent electromagnetic relativistic code with mobile ions. The numerical algorithm used in the code follows that in Ref. [18]. In the simulations, the short pulse laser has a wavelength $\lambda_1 = 800$ nm, a peak intensity $I_1 = 10^{16}$ W/cm^2 (a typical value), and linear polarization. The normalized field amplitude is $a_1 = 0.068$, which is defined as $a_j = eE_j/m_e\omega_j c$ where E_j and ω_j are the laser electric field and the angular frequency, respectively. The pulse shape is Gaussian and the pulse length is $L_1 = 10\lambda_1$ (a full width at e^{-1} of the electric field). The parameters of the long pulse laser are a wavelength $\lambda_2 = 700-1000$ nm, a peak intensity $I_2 = 10^{14}-10^{17}$ W/cm^2, and linear polarization identical to the short pulse. The long pulse has a flat top given by a super-Gaussian shape of $\exp[-(x/0.5L_2)^{16}]$ and the pulse length is $L_2 = 160\lambda_2$. The plasma consists of electrons and ions with an ion mass of $m_i = 1836 m_e$. Initially, the particles are placed in a plasma layer of width $120\lambda_1$ with a uniform profile. Two vacuum regions bound this plasma layer. The two pulses propagate from the vacuum regions into the plasma region in the counter direction. In the standard simulations, the spatial mesh size is $0.1\lambda_1$ and the number of particles is 4×10^5 for each species. Particle-particle collisions are not included. This is a proper assumption because the electron-ion collision frequency (which is evaluated from the quivering velocity in the laser field) is several orders of magnitude smaller than the plasma frequency.

Figure 1 shows the temporal behavior of the laser field and the excited wake field. The laser parameters are $\lambda_1 = 800$ nm, $\lambda_2 = 727$ nm, $I_1 = I_2 = 10^{16}$ W/cm^2, and the electron density is 3.5×10^{18} cm^{-3} ($n_e/n_{\mathrm{cr}} = 0.002$ where n_{cr} is the critical density defined as $n_{\mathrm{cr}} = m_e\varepsilon_0\omega_1^2/e^2$). The plasma frequency is $\omega_p/\omega_1 = 0.045$. Figures 1(a) and 1(b) are the initial wave pattern and the plasma density profile. When the two beams collide [Fig. 1(c)], a large density fluctuation, of

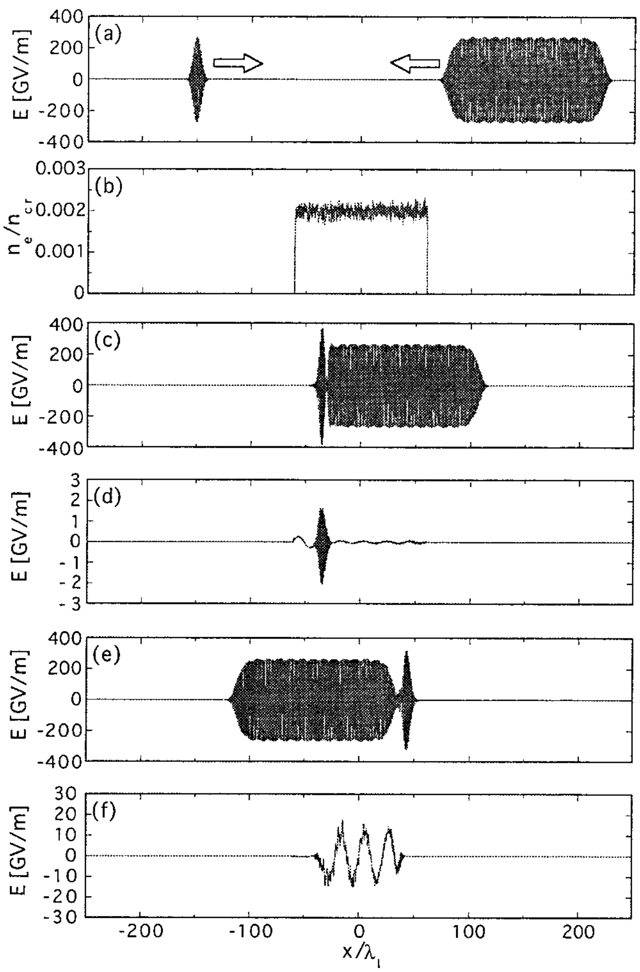

FIG. 1. Profiles of the laser fields (a), (c), and (e), the excited wake fields (d) and (f), and the electron density (b). The parameters of the two laser pulses are $\lambda_1 = 800$ nm, $\lambda_2 = 727$ nm, and $I_1 = I_2 = 10^{16}$ W/cm^2, and the electron density is 3.5×10^{18} cm^{-3}. Figures (a) and (b) are the initial laser field pattern and the plasma density profile. Figures (c) and (d) are the laser field and the longitudinal electric field when the two beams collide. Figures (e) and (f) are those when the two beams pass through.

which the wave number is $k_1 + k_2$, is generated in the interference region. This density fluctuation induces a longitudinal electric field fluctuation, as can be seen in Fig. 1(d). A standard LWF is observed behind the short pulse laser [on the left-hand side of the interference region shown in Fig. 1(d)]. The long pulse laser also induces a small amplitude LWF (on the right-hand side of the interference region). It is excited by the front edge gradient of the long pulse laser. The enhanced wake field grows in the interference region and it is continuously excited behind the short pulse laser, apparently similar to the standard LWF [Fig. 1(b)]. However, the field amplitude of the enhanced wake is a factor of 40 greater than that of the standard one. After the two laser interaction, the laser field of the short pulse becomes a bit larger than the initial field [Fig. 1(e)]. This is due to parametric amplification in the plasma media [19].

The detailed behavior of the enhanced wake field is compared with that of the standard LWF. Figure 2 shows wave

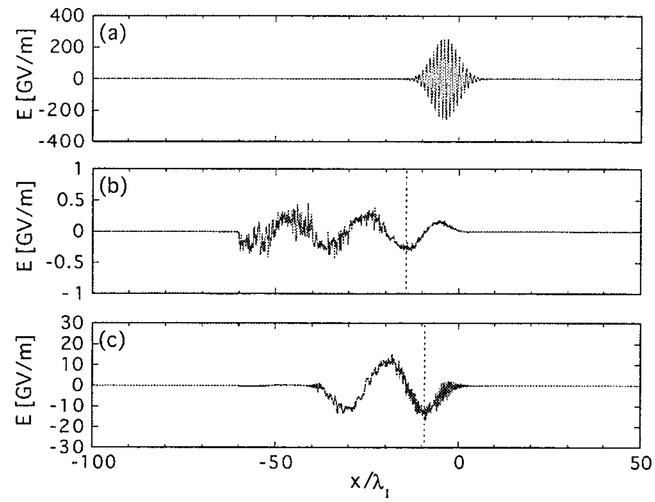

FIG. 2. Wave forms of the short pulse laser (a), the standard LWF (b), which is excited by only the short pulse laser, and the enhanced wake field generated by the two pulses (c). The parameters of the two laser pulses are $\lambda_1 = 800$ nm, $\lambda_2 = 727$ nm, and $I_1 = I_2 = 10^{16}$ W/cm^2, and the electron density is 3.5×10^{18} cm^{-3}.

forms of the short pulse laser (a), the standard LWF (b), and the enhanced wake field generated by the two colliding beams (c), where the plasma region is $-60 \leq x/\lambda_1 \leq +60$ and the counterpropagating long pulse laser is not shown. In the calculation the same parameters are used as those of Fig. 1. It is observed that the phase of the wake fields between the standard one and the enhanced one differ by about $\pi/2$ in this case. This result is the same as that in the recent work [20], where the phase relation was examined in detail and pointed out that the phase of the enhanced wake depends on the sign of the frequency detuning between the two laser beams.

The wake field amplitude generated by the two colliding laser beams increases with the laser intensities, which was examined theoretically in a linear slow wave regime [16]. Figure 3 shows the dependence of the wake field amplitude on the laser intensities. The intensities are varied in the range of $I_1 = 0.25\times10^{16}$ to 4×10^{16} W/cm^2 ($a_1 = 0.034$–0.14) and $I_2 = 0.02\times10^{16}$ to 5×10^{16} W/cm^2 ($a_2 = 0.009$–0.14). In the lower intensity range of $a_1\times a_2 < 0.004$, the field amplitude increases in proportion to $(a_1\times a_2)^2 \propto I_1\times I_2$, as explained from the linear theory [16]. The amplitude saturates in the high intensity range and the value is about 12 GV/m. From the theoretical analysis [20], the saturation level is ω_p/ω_1 of the wave breaking limit, $E_{\mathrm{wb}} = m_e c\omega_p/e$ [21]. In this case, the wave breaking limit is evaluated to be 180 GV/m and the saturation level is 0.067. Therefore, the saturated amplitude is consistent with the above theory. This largest amplitude in the saturated state would be used in real applications, such as particle accelerators. Therefore, it is important to know the behavior of the wake field in the saturated regime, in particular, the dependence of the field amplitude on the frequency difference between the two colliding laser beams.

This dependence of the field amplitude on the laser frequency is examined by varying the frequency of the long pulse laser, ω_2, as shown in Fig. 4 (where the frequency difference is defined as $\Delta\omega = \omega_2 - \omega_1$). The calculation pa-

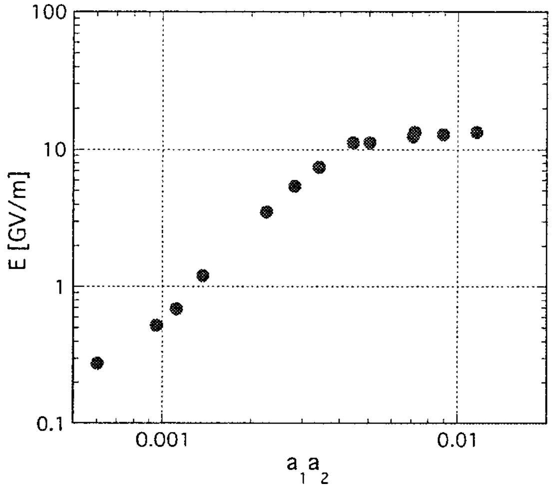

FIG. 3. Dependence of the excited wake field amplitude on the laser intensities. The intensities are varied in the range of $I_1 = 0.25\times 10^{16}$ to $4\times 10^{16}\,\mathrm{W/cm^2}$ ($a_1 = 0.034$–0.14) and $I_2 = 0.02\times 10^{16}$ to $5\times 10^{16}\,\mathrm{W/cm^2}$ ($a_2 = 0.009$–0.14). The other parameters are $\lambda_1 = 800$ nm, $\lambda_2 = 727$ nm, and $n_e = 3.5\times 10^{18}\,\mathrm{cm^{-3}}$.

rameters are the same as those of Fig. 1, except for ω_2. As the laser intensities are $a_1\times a_2 = 0.005$, this wake field is in the saturated regime. If the long pulse laser is absent, the field amplitude (the standard LWF) is about 0.3 GV/m, which is consistent with the theoretical evaluation [22]. When the frequency difference is zero ($\omega_1 = \omega_2$), the field amplitude is approximately equal to the standard one. The enhanced wake field is observed in both cases of $\omega_2 > \omega_1$ and $\omega_2 < \omega_1$. The enhancement is observed in broad frequency ranges ($\Delta\omega \approx \pm 0.2\omega_1$). The peaks of the field amplitude are located at $\Delta\omega \approx \pm 0.1\omega_1$, which is a factor of about 2 larger than the plasma frequency $\omega_p = 0.045\omega_1$. This frequency relation, $\Delta\omega \approx \pm 2\omega_p$, at the maximum field amplitude in the saturated regime is remarkably different from that in the linear regime, where the field amplitude becomes maximum at $\Delta\omega = \pm 1.1\omega_p$ [16].

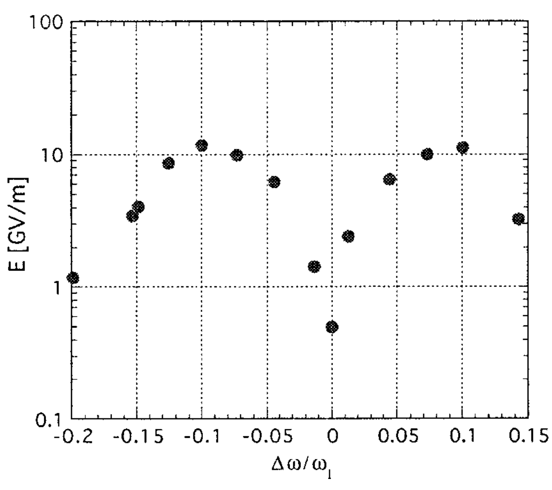

FIG. 4. Dependence of the excited wake field amplitude on the frequency difference of the two laser pulses (the frequency difference is defined as $\Delta\omega \equiv \omega_2 - \omega_1$). The simulation parameters are $I_1 = I_2 = 10^{16}\,\mathrm{W/cm^2}$ and $n_e = 3.5\times 10^{18}\,\mathrm{cm^{-3}}$.

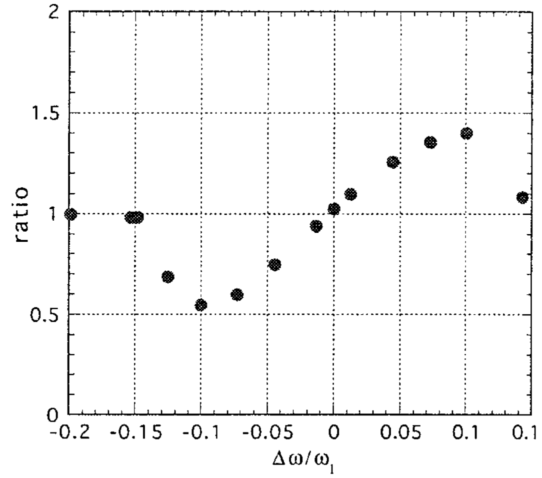

FIG. 5. Ratio of the short pulse laser energy after the interaction with respect to the initial energy as a function of the frequency difference. The simulation parameters are $I_1 = I_2 = 10^{16}\,\mathrm{W/cm^2}$ and $n_e = 3.5\times 10^{18}\,\mathrm{cm^{-3}}$.

As mentioned above, the parametric process (Raman back scattering) amplifies the laser pulse. In general, the parametric process occurs with resonance conditions of $\omega_2 - \omega_1 = \pm\omega_p$ and $\mathbf{k}_2 - \mathbf{k}_1 = \pm\mathbf{k}_p$. The short pulse laser, of which frequency is ω_1 in this paper, is amplified when $\omega_2 > \omega_1$ and decays when $\omega_2 < \omega_1$. In this case, the resonance condition for the plasma wave excitation does not need to be satisfied precisely [19]. From our numerical results, the frequency dependence is clearly observed as shown in Fig. 5, where the ratio of the short pulse laser energy (the pulse energy after the interaction over the initial energy) is plotted as a function of the frequency difference. The short pulse energy increases when $\omega_2 > \omega_1$ and decreases when $\omega_2 < \omega_1$. The peaks of the change are located at $\Delta\omega/\omega_1 = \pm 0.1$ in spite of $\omega_p/\omega_1 = 0.045$. This frequency relation is identical with that of the enhanced wake amplitude as shown in Fig. 4. In these calculations, the laser pulse energy is depleted from the excitation of the wake field for both $\omega_2 > \omega_1$ and $\omega_2 < \omega_1$. For example, in the case of Fig. 1, the energy of the excited wake field is about 2% of the short pulse laser energy, which is considerably smaller than the change of the laser energy due to the parametric process.

In conclusion, the enhanced laser wake field, which is generated using two colliding laser beams, was examined numerically, concentrating on the frequency dependence in the saturated regime. It was found that the frequency relation in the saturated regime is remarkably different from that in the linear regime. This enhanced wake field is obtained from the moderate experimental conditions, where the laser intensities are relatively low ($\sim 10^{16}\,\mathrm{W/cm^2}$) and no precise frequency tuning is needed. Therefore, it is attractive as a scheme for laser-driven acceleration or plasma micro-undulator [23].

It is a pleasure to acknowledge the support of the staff at the Advanced Photon Research Center. The authors would like to thank Dr. Y. Kato for his many helpful comments.

[1] T. Tajima and J. M. Dawson, Phys. Rev. Lett. **43**, 267 (1979).
[2] C. E. Clayton *et al.*, Phys. Rev. Lett. **70**, 37 (1993).
[3] F. Amiranoff *et al.*, Phys. Rev. Lett. **74**, 5220 (1995).
[4] F. Amiranoff *et al.*, Phys. Rev. Lett. **81**, 995 (1998).
[5] K. Nakajima *et al.*, Phys. Rev. Lett. **74**, 4428 (1995).
[6] D. Umstadter *et al.*, Science **273**, 472 (1996).
[7] R. Wagner *et al.*, Phys. Rev. Lett. **78**, 3125 (1997).
[8] A. Ting *et al.*, Phys. Plasmas **4**, 1889 (1997).
[9] D. Gordon *et al.*, Phys. Rev. Lett. **80**, 2133 (1998).
[10] J. R. Marques *et al.*, Phys. Rev. Lett. **76**, 3566 (1996); J. R. Marques *et al.*, Phys. Plasmas **5**, 1162 (1998).
[11] C. W. Siders *et al.*, Phys. Rev. Lett. **76**, 3570 (1996).
[12] A. Ting *et al.*, Phys. Rev. Lett. **77**, 5377 (1996).
[13] P. Sprangle *et al.*, Phys. Rev. Lett. **69**, 2200 (1992).
[14] T. M. Antonsen, Jr. and P. Mora, Phys. Rev. Lett. **69**, 2204 (1992).
[15] W. B. Mori *et al.*, Phys. Rev. Lett. **72**, 1482 (1994).
[16] G. Shvets *et al.*, Phys. Rev. E **60**, 2218 (1999).
[17] K. Nagashima, Y. Kishimoto, and H. Takuma, Phys. Rev. E **58**, 4937 (1998).
[18] C. K. Birdsall and A. B. Langdon, *Plasma Physics via Computer Simulation* (McGraw-Hill, New York, 1985).
[19] G. Shvets *et al.*, Phys. Rev. Lett. **81**, 4879 (1998).
[20] G. Shvets, N. J. Fisch, and A. Pukhov, IEEE Trans. Plasma Sci. **28**, 1194 (2000).
[21] A. I. Akhiezer and R. V. Polovin, Sov. Phys. JETP **3**, 696 (1956); J. M. Dawson, Phys. Rev. **113**, 383 (1959); Z. M. Sheng and J. Meyer-ter-Vehn, Phys. Plasmas **4**, 493 (1997).
[22] P. Sprangle and E. Esarey, Phys. Fluids B **4**, 2241 (1992).
[23] C. Joshi *et al.*, IEEE J. Quantum Electron. **23**, 1571 (1987).